

See discussions, stats, and author profiles for this publication at: <https://www.researchgate.net/publication/346554278>

An analytical solution for rapidly predicting post-fire peak streamflow for small watersheds in southern California

Article in *Hydrological Processes* · December 2020

DOI: 10.1002/hyp.13976

CITATIONS

0

READS

57

10 authors, including:



Brenton A. Wilder

San Diego State University

2 PUBLICATIONS 0 CITATIONS

[SEE PROFILE](#)



Peter H. Cafferata

State of California

39 PUBLICATIONS 133 CITATIONS

[SEE PROFILE](#)



Drew Coe

California Department of Forestry and Fire Protection (CAL FIRE)

25 PUBLICATIONS 233 CITATIONS

[SEE PROFILE](#)



Bill Short

Californian Department of Conservation

16 PUBLICATIONS 15 CITATIONS

[SEE PROFILE](#)

Some of the authors of this publication are also working on these related projects:





The Effects of Post-Fire Forest Management on Runoff and Erosion in the Coast Range of Northern California [View project](#)



Watercourse crossing design [View project](#)

An analytical solution for rapidly predicting post-fire peak streamflow for small watersheds in southern California

Brenton A. Wilder¹  | Jeremy T. Lancaster² | Peter H. Cafferata³ |
Drew B. R. Coe³ | Brian J. Swanson⁴ | Donald N. Lindsay⁵ | William R. Short² |
Alicia M. Kinoshita¹ 

¹Department of Civil, Construction, and Environmental Engineering, San Diego State University, San Diego, California, USA

²Department of Conservation - California Geological Survey, Sacramento, California, USA

³California Department of Forestry and Fire Protection, Sacramento, California, USA

⁴Department of Conservation - California Geological Survey, Los Angeles, California, USA

⁵Department of Conservation - California Geological Survey, Redding, California, USA

Correspondence

Alicia M. Kinoshita, Department of Civil, Construction, and Environmental Engineering, San Diego State University, 5500 Campanile Drive, San Diego, CA 92182-1324, USA.
Email: akinoshita@sdsu.edu

Funding information

Joint Fire Science Program Graduate Research Innovation Award, Grant/Award Number: #19-1-01-55; San Diego State University, Grant/Award Number: Master's Research Scholarship; Department of Conservation - California Geological Survey

Abstract

Following wildfires, the probability of flooding and debris flows increase, posing risks to human lives, downstream communities, infrastructure, and ecosystems. In southern California (USA), the Rowe, Countryman, and Storey (RCS) 1949 methodology is an empirical method that is used to rapidly estimate post-fire peak streamflow. We re-evaluated the accuracy of RCS for 33 watersheds under current conditions. Pre-fire peak streamflow prediction performance was low, where the average R^2 was 0.29 and average RMSE was 1.10 cms/km² for the 2- and 10-year recurrence interval events, respectively. Post-fire, RCS performance was also low, with an average R^2 of 0.26 and RMSE of 15.77 cms/km² for the 2- and 10-year events. We demonstrated that RCS overgeneralizes watershed processes and does not adequately represent the spatial and temporal variability in systems affected by wildfire and extreme weather events and often underpredicted peak streamflow without sediment bulking factors. A novel application of machine learning was used to identify critical watershed characteristics including local physiography, land cover, geology, slope, aspect, rainfall intensity, and soil burn severity, resulting in two random forest models with 45 and five parameters (RF-45 and RF-5, respectively) to predict post-fire peak streamflow. RF-45 and RF-5 performed better than the RCS method; however, they demonstrated the importance and reliance on data availability. The important parameters identified by the machine learning techniques were used to create a three-dimensional polynomial function to calculate post-fire peak streamflow in small catchments in southern California during the first year after fire ($R^2 = 0.82$; RMSE = 6.59 cms/km²) which can be used as an interim tool by post-fire risk assessment teams. We conclude that a significant increase in data collection of high temporal and spatial resolution rainfall intensity, streamflow, and sediment loading in channels will help to guide future model development to quantify post-fire flood risk.

KEYWORDS

flooding, post-fire peak streamflow, random forest, Rowe, Countryman, and Storey, wildfire

1 | INTRODUCTION TO POST-FIRE HAZARDS IN SOUTHERN CALIFORNIA

Anthropogenic climate change, human ignited fires, and increased fuel loads resulting from decades of fire suppression in forested areas have contributed to an increase in wildfire severity and occurrence in the western U.S. (FRAP, 2018; Radeloff et al., 2005; Westerling et al., 2006). These wildfires can significantly impact land cover and soil properties (DeBano, 2000; Moody, 2012; Moody & Martin, 2001; Neary et al., 2005; Rowe et al., 1949) and can pose risks to human lives, valued assets, and ecosystems (Kinoshita et al., 2016; Shakesby et al., 2016). Development in wildlands and at the wildland-urban interface has further exacerbated the potential to impact communities. In California, extreme increases in peak streamflow after wildfire contribute to catastrophic flooding and debris flows on steep alluvial fan landforms that may be developed with suburbs and infrastructure.

For example, the Holy Fire (August 2018) burned about 94 km² in Orange County and Riverside County in California and affected over 1000 residents. Three months later, the Woolsey and Hill fires (November 2018) burned approximately 392 km² in Los Angeles County and Ventura County. Combined, these two fires resulted in three fatalities, eight non-fatal injuries, and 1665 structures being destroyed. Quickly following these wildfires (December 2018–February 2019), record amounts of rainfall resulted in flooding and debris flows in the burned regions. During this time, the Riverside County Fire Department ordered the evacuation of 300 homes. Furthermore, on 9 January 2018, while the Thomas Fire was still burning, Santa Barbara County was impacted by post-fire debris flows that killed 23 people, destroyed or damaged 558 structures, and caused severe damage to infrastructure in Montecito and Carpinteria, California (Kean et al., 2019; Lancaster et al., in press).

Federal, state, and local agencies rapidly assess burned watersheds to produce timely emergency protection measures for nearby communities that may be in the immediate danger from elevated peak flows and debris flows. Federal Burned Area Emergency Response (BAER) teams and California State Watershed Emergency Response Teams (WERTs) are reliant on modelling to make informed decisions (Foltz et al., 2009) following field verification of soil burn severity categories (Parsons et al., 2010). The models used to predict these processes have varying degrees of sophistication (Cannon et al., 2004; Kinoshita et al., 2014; Robichaud et al., 2007). Debris flows, debris yields, and surface erosion estimates are based on either numerical modelling (Water Erosion Prediction Project derivatives) or relatively robust empirical models, where the independent variables are consistent with our physical understanding of geomorphic processes (Gartner et al., 2014; Robichaud et al., 2011; Staley et al., 2017). WERTs and BAER teams inventory values-at-risk (VARs) and suggest emergency protection measures that can be rapidly implemented, including early warning system use, storm patrol, structure protection with sandbags or K-rails, channel clearance work near crossings, signage to close low water crossings, parks and trails, and road crossing upgrades (Foltz et al., 2009). Emergency response teams also rapidly communicate VAR locations and emergency protection measures to local agencies such as county department of public works and flood control districts for implementation.

Accurate predictions of post-fire peak streamflow rates are critical for key emergency response and management agencies such as the California Department of Forestry and Fire Protection (CAL FIRE), California Department of Conservation-California Geological Survey (CGS), the U.S. Forest Service (USFS), and local county flood control districts especially under changing climate and wildfire regimes. Peak fire season in southern California occurs in the fall, creating a short period between fire and winter storms that produce flood events. This pattern requires effective hazard evaluation to minimize risk for downstream communities, infrastructure, and ecosystems. Further, evidence suggests that California's peak fire season could be shifting later in the year to November–December due to climate change affecting coastal temperature, air pressure, and humidity (N. L. Miller & Schlegel, 2006). This emphasizes the urgency for federal, state, and local agencies to rapidly assess burned watersheds and produce timely emergency protection measures for nearby communities.

Post-fire peak streamflow can exceed unburned peak streamflow by three orders of magnitude during similar pre-fire storm events (Moody & Martin, 2001; Wagenbrenner, 2013; Wohlgemuth, 2016). In southern California, there is substantial reliance on the look-up-tables (LUTs) developed by Rowe et al. (1949) to predict post-fire peak flows. This simpler method is well understood and convenient for rapid assessment in comparison to more complex process-based hydrologic models, and therefore, is the most widely used method for rapidly predicting post-fire peak flow rates in southern California (Kinoshita et al., 2014). Notable fires such as the 2003 Old and Grand Prix Fires, 2009 Station Fire, 2018 Holy Fire, 2018 Woolsey and Hill fires, 2019 Saddle Ridge Fire, and 2019 Cave Fire have utilized the Rowe, Countryman, and Storey (RCS) methods for post-fire peak streamflow predictions (e.g., Biddinger et al., 2003; Moore et al., 2009; WERT, 2018a, 2018b, 2019a, 2019b). It is hypothesized that the RCS model does not accurately predict post-fire peak streamflow at the small to medium watershed scale (1 to 50 km²), a common scale needed for post-fire risk assessment.

Building upon the significant advances in post-fire hydrology since the development of RCS, there is an opportunity to improve current methodologies for prediction of peak streamflow in small watersheds. In particular, machine learning techniques can be used for post-fire applications (Saxe et al., 2018; Schmidt et al., 2020). Saxe et al. (2018) utilized machine learning to study a vast area with varying watershed scales. Our study focuses on small to medium-sized watersheds ranging from 1 to 42 km² to reduce error associated with scaling, and to improve regional responses when using machine learning. To evaluate and improve the accuracy of decision support tools for post-fire hazard prediction and management in southern California, we 1) assess the validity of the RCS method using observed pre- and post-fire peak streamflow, 2) identify important parameters that can improve the characterization of post-fire responses using machine learning, and 3) present an analytical tool for post-fire risk assessments.

2 | STUDY AREA

The study area is within the Transverse Ranges and Peninsular Ranges, which are geomorphic provinces with a wide topographic

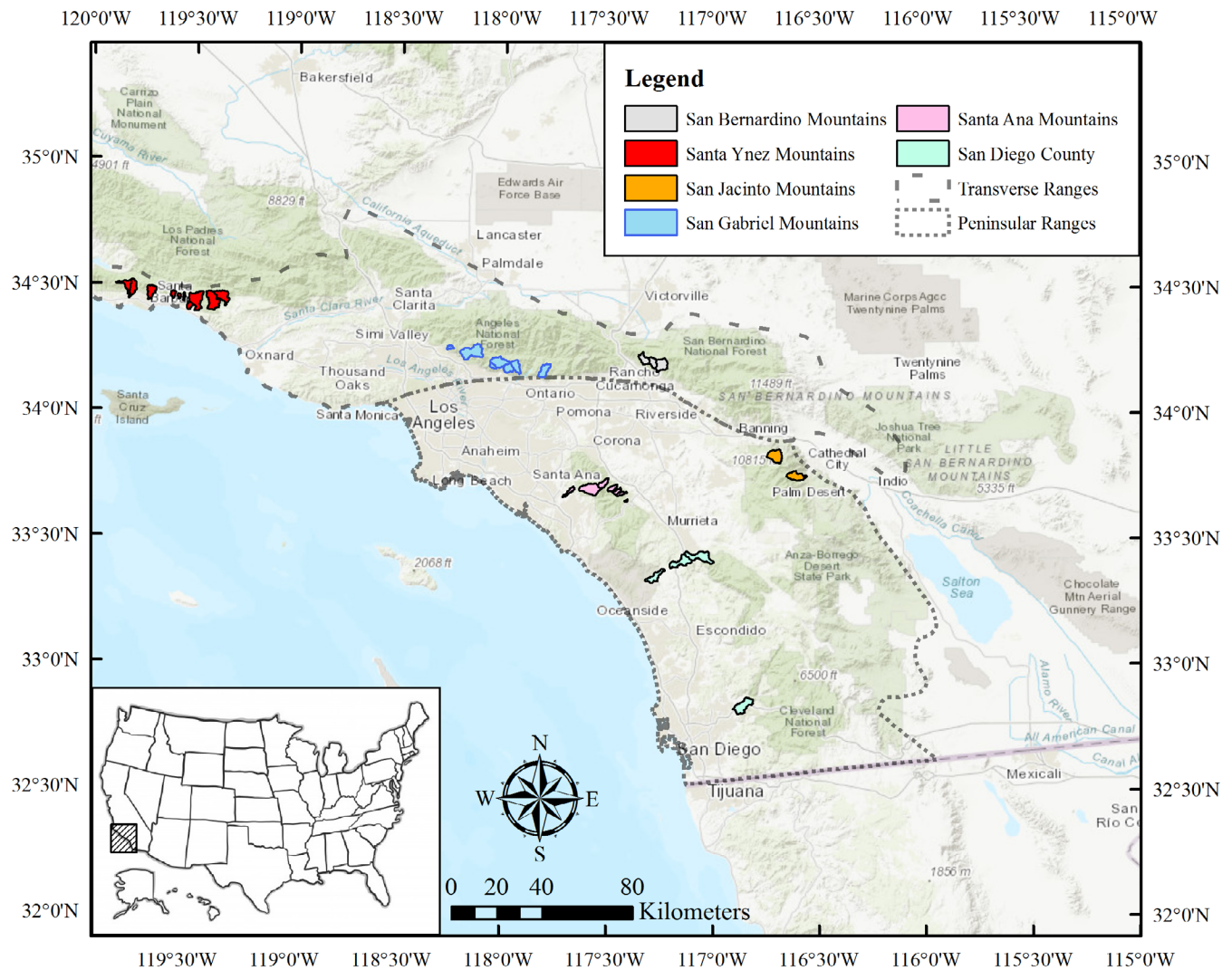


FIGURE 1 Study area consisted of 33 watersheds in 6 different regions within the Transverse Ranges and Peninsular Ranges in southern California, USA

range from sea level to 3506 m (CGS, 2002). The study area straddles the southern California Coastal and southern California Mountain and Valleys ecoregions (Cleland et al., 2007). Approximately 60%–70% of these ecoregions are dominated by shrubland (e.g., chaparral) vegetation types, with a lesser proportion occupied by grassland and woodland or forest vegetation types (FRAP, 2015). The median pre-settlement fire return intervals for these vegetation types are variable, ranging on average from approximately 60 to 100 years for chaparral and coastal scrub vegetation types (Van de Water & Safford, 2011). This research investigated 33 small- to medium-sized watersheds with drainage areas ranging between 1.2 to 41.7 km² (Figure 1; Table 1).

2.1 | Regional geology

The Transverse Ranges are characterized by a 480-km long east-west-trending series of steep mountain ranges, which include the Santa Ynez, San Gabriel, and San Bernardino mountains in the study

area. They are underlain by diverse rock types of different ages. Older Precambrian to Cretaceous metamorphic and igneous rocks underlie the western San Bernardino and central San Gabriel mountains (CGS, 2018). In contrast, the Santa Ynez Mountains are underlain by younger marine and continental sedimentary sequences of sandstone, siltstone, and shale, deposited during late Cretaceous and Cenozoic times (CGS, 2018).

The Peninsular Ranges are characterized by a series of northwest-trending mountain ranges, including the Santa Ana, San Jacinto, and Laguna mountains, having generally lower average elevation than the Transverse Ranges. They are characterized by igneous and metamorphic rocks of Mesozoic age, including granite in the east and volcanic and metasedimentary rocks in the west (CGS, 2018; Harden & Matti, 1989).

Mountain ranges in these provinces have steep canyons with active hillslope processes including shallow and deep-seated landslides, rockfall, and debris flow initiation. Pleistocene- and Holocene-age alluvial and debris fan landforms deposited at the mountain front

TABLE 1 Study watershed characteristics (name, size, wildfire, and burn severity) by region, where burn severity is categorized by Unburned-Low (Un-Low), moderate (Mod), and high (High)

Watershed Name (RCS Table No.)	Size (km ²)	Wildfire (% Burned Area)	Un-Low (%)	Mod (%)	High (%)
San Bernardino Mountains					
Devil (60)	14.2	2003 Old (97%)	50%	31%	19%
East Twin Creek (57)	22.6	2003 Old (98%)	50%	31%	19%
Waterman (58)	11.9	1980 Panorama (86%)	n/a	n/a	n/a
Santa Ynez Mountains					
Maria Ygnacio (204)	16.6	1990 Painted Cave (52%)	65%	26%	9%
Franklin (188)	6.9	1971 Romero (56%)	n/a	n/a	n/a
Coyote (183)	33.9	1985 Wheeler (98%)	39%	33%	28%
Mission (200)	17.1	2009 Jesusita (69%)	60%	32%	8%
San Jose (205)	14.4	1955 Refugio (69%)	n/a	n/a	n/a
Carpinteria (187)	33.9	1971 Romero (84%)	n/a	n/a	n/a
Santa Ana (182)	24.2	1985 Wheeler (100%)	39%	33%	28%
Romero (193)	5.14	2017 Thomas Fire (94%)	59%	39%	2%
Toro (190)	2.33	2017 Thomas Fire (94%)	59%	39%	2%
Arroyo Paredon (191)	2.22	2017 Thomas Fire (83%)	59%	39%	2%
San Jacinto Mountains					
Snow (85)	27.9	1973 One Horse (37%)	n/a	n/a	n/a
Andreas (82)	22.4	1980 Dry Falls (92%)	n/a	n/a	n/a
		2013 Mountain Fire (67%)	49%	49%	2%
San Gabriel Mountains					
Little Santa Anita (136)	4.8	1954 Monrovia Peak (100%)	n/a	n/a	n/a
Sawpit (131)	13.7	1924 San Gabriel #2 (73%)	n/a	n/a	n/a
Fish (129)	18.3	1968 Canyon Inn (100%)	n/a	n/a	n/a
Lower Big Dalton (117)	18.8	1919 San Gabriel (100%)	n/a	n/a	n/a
Haines (145)	3.3	1933 La Crescenta (51%)	n/a	n/a	n/a
Arroyo Seco (141)	41.7	2009 Station (100%)	34%	38%	28%
Santa Anita (137)	25.2	1954 Monrovia Peak (97%)	n/a	n/a	n/a
Santa Ana Mountains					
Horsethief (35)	5.6	2018 Holy (100%)	15%	71%	14%
Indian (35)	7.3	2018 Holy (100%)	15%	71%	14%
Rice (35)	5	2018 Holy (100%)	15%	71%	14%
Dickey (34)	1.2	2018 Holy (98%)	15%	71%	14%
Coldwater (36)	10.7	2018 Holy (99%)	15%	71%	14%
Agua Chinon (32)	7.1	2007 Santiago (92%)	61%	28%	11%
Santiago (32)	32.3	2007 Santiago (70%)	61%	28%	11%
San Diego County					
Los Coches (14)	31.6	2003 Cedar (57%)	24%	24%	52%
Pechanga (28)	34.6	2000 Pechanga (45%)	32%	34%	34%
Fallbrook (27)	18.3	2014 Tomahawk (59%)	42%	52%	6%
Rainbow (27)	26.7	2007 Rice (20%)	75%	17%	8%

Note: Note that burn severity data collected from monitoring trends in burn severity (MTBS) are not available for fires prior to 1984, which are indicated by n/a.

throughout these provinces demonstrate dominant watershed runoff and sedimentation processes ranging from sediment-laden stream flows to debris flows.

At the catchment scale, many geologic factors control sediment availability in the region. These include rock type (lithology), structure, presence of landslides, weathering characteristics, elevation, slope,

and tectonic history (DiBiase & Lamb, 2020; Lavé & Burbank, 2004; Scott & Williams, 1978). Rock to regolith conversion is rapid in the study area, thus, shallow landslides, dry ravel, and rill erosion after wildfire may dominate the sediment supply. Conversely, where regolith conversion is slow, deep-seated landslides may dominate hillslope processes with landslide deposits and their over-steepened source areas as primary sediment sources. To represent this in our model, soil erodibility factors and landslide susceptibility maps were used as parameters for analysis.

2.2 | Climate and wildfire

The Transverse Ranges and Peninsular Ranges experience some of the highest storm precipitation totals in the nation (Dettinger, 2011; O'Connor & Costa, 2004; Ralph & Dettinger, 2012). Further, the unique east-west alignment of the Transverse Ranges relative to the Pacific Ocean translates to large amounts of orographic precipitation from atmospheric rivers, where 10%–30% of the annual precipitation can originate from one large storm (Lamjiri et al., 2018) during cool season months of November–April (Dettinger, 2011; Neiman et al., 2008).

Multi-year drought interspersed with, or followed by, extreme precipitation or wetter than average years are common in the area, a pattern conducive to growth and then desiccation of the region's fire-prone vegetation. The combination of steep and complex terrain, combustible fuels, prolonged dry seasons, and strong Santa Ana wind events produce the most intense fire climate in the United States (Keeley et al., 2004; Raphael, 2003; Wells, 1987; Wells II., 1981). Further, population growth proximal to wildlands means that much of southern California has experienced higher fire frequency relative to pre-settlement return intervals (Safford & Van de Water, 2014; Syphard et al., 2007).

While southern California's chaparral and forested ecosystems are fire-adapted, climate change is predicted to increase mean annual burned area by 42% for forests in the San Gabriel Mountains under RCP 8.5 scenario (Representative Concentration Pathways) between the initial period of 1950 to 2005 and the projected period of 2006 to 2099 (<https://cal-adapt.org/>). One study observed no apparent increase in summer wildfire in non-forested areas between 1972 to 2018, however, observed a slight increase in fall wildfire probability due to atmospheric aridity (Williams et al., 2019), which is exemplified by the fall fires in 2017 and 2018, including the 2017 Thomas Fire, the largest wildfire documented in southern California.

2.3 | Post-fire processes

The regional climatology, geology, soils, and vegetation in southern California equates to an unmatched magnitude of post-fire hydrogeomorphic response (Moody et al., 2013). Examples of extreme impacts include the 1934 New Year's Day debris flow in the La Crescenta area (Chawner, 1935); the 1981 Mill Creek disaster in the San Gabriel Mountains (Shuirman & Slosson, 1992); the December

25th debris flows following the 2003 Old Fire (Cannon & DeGraff, 2009); and, hyperconcentrated flood flows following the 2018 Holy Fire causing damage to homes, flood control facilities, and highway infrastructure in (and below) the Santa Ana Mountains. For example, observed hyperconcentrated flood flow velocities varied greatly by watershed during the 29 November 2018 storm following the 2018 Holy Fire with flows at Dickey Canyon producing a flow velocity of approximately 12 m/s, Rice, Horethief, and Indian Canyons producing flow velocities between 5–8 m/s, and Coldwater Canyon producing a flow velocity of approximately 3 m/s. Short duration, high intensity precipitation produced from atmospheric rivers and orographic lift is a key factor that generates flash floods and debris flows after wildfire (Cannon et al., 2008; Moody et al., 2013; Oakley et al., 2017). Moreover, precipitation intensity is anticipated to increase about 7% per degree Celsius of warming, suggesting a potential increase of flash flood and debris flow magnitude after wildfire in a changing climate (Prein et al., 2017).

In southern California, the dominant vegetation types covering the hills and lower mountain slopes are the chaparral and scrub brushes. Further, the closed canopy nature of these vegetation types means that large scale, stand-replacing fires are common (Keeley, 2009). After stand-replacing fires on steep slopes, dry ravel increases, with much of it delivered directly into the channel network resulting in large increases in sediment yield and/or the frequency of debris flows (DiBiase & Lamb, 2020). Since post-fire runoff reflects a continuum between clear water flow and debris flows (non-Newtonian fluid), the recognition of these linked processes is vital for understanding the fire-flood cycle in southern California (Travis et al., 2012). The well-established linkage between chaparral vegetation and the development of soil water repellency (DeBano, 2000; Doerr et al., 2000) influences infiltration, runoff, and erosion (Doerr et al., 2009). Soil water repellency and soil erosion are enhanced with increasing soil burn severity (Huffman et al., 2001; Lewis et al., 2006) due to changes in mechanical and hydraulic properties such as changes in relative density, saturated hydraulic conductivity, and sorptivity (Shakesby et al., 2016). Thus, soil burn severity is crucial for modelling of hydrologic response after wildfire in southern California.

3 | METHODS

3.1 | Data

To develop the random forest (RF) (Breiman, 2001) algorithm to characterize historical post-fire peak streamflow in southern California, 45 watershed parameters (Table S1) were derived from local and national data bases. These sources included streamflow records from the United States Geological Survey (USGS), hourly precipitation data from National Oceanic and Atmospheric Administration (NOAA), the average annual precipitation (USGS StreamStats), burn perimeters and severity from Monitoring Trends in Burn Severity (MTBS), soils data from the USDA Natural Resources Conservation Service's Soil Survey Geographic Database (SSURGO), land cover data from the National Land Cover Database (NLCD), and digital elevation models (DEM) from USGS Elevation Products. Selection of these parameters were

based on a review of studies that directly linked the effects of specific parameters on pre- and post-fire processes. Some of the datasets were not available for all post-fire events, specifically, burn severity datasets were only available after 1984.

3.2 | Performance measurements

To measure model performance, the following statistics were used to estimate the bias, root mean squared error (RMSE), and coefficient of determination (R^2):

$$\text{Bias} = \frac{1}{n} \sum_{i=1}^n (P_i - O_i) \quad (1)$$

$$\text{RMSE} = \sqrt{\sum_{i=1}^n \frac{(P_i - O_i)^2}{n}}, \quad (2)$$

where n is the number of watersheds, i is the i -th watershed, O_i is observed peak streamflow for i -th watershed, and P_i is predicted peak streamflow for i -th watershed. Positive bias represents an overprediction and a negative bias represents an underprediction. Higher RMSE values are associated with higher error than those with lower RMSE values.

$$R^2 = 1 - \frac{\sum_{i=1}^n (e_i)^2}{\sum_{i=1}^n (y_i - \bar{y})^2}, \quad (3)$$

where e_i is error at point i , y_i known streamflow at point i , and \bar{y} is average streamflow. Higher R^2 values that are closer to 1, or equal to 1, represent higher agreement between the predicted and observed values.

3.3 | Peak streamflow modelling methods

3.3.1 | Flood frequency of historical flows

RCS-derived pre- and post-fire predictions were compared to historical streamflow records. The observed peak streamflow values are based on statistical distributions and not individual observations. Weibull and PeakFQ were used to estimate flood frequency for existing streamflow records (Clarke, 2002; Flynn et al., 2006). Weibull is a generalization of the exponential distribution to calculate peak streamflow for different flood frequencies:

$$T = \frac{n+1}{m}, \quad (4)$$

where T is return period in years, n , is the number of data points and, m , is the rank of highest annual streamflow. The Peak FQ program was developed by the USGS and utilizes a log-Pearson Type III distribution to model flood frequencies, based on Bulletin 17C (Parrett et al., 2011) procedures:

$$\log Q = \bar{x} + S \times k, \quad (5)$$

where $\log Q$, is the logarithmic peak streamflow, \bar{x} , is the sample logarithmic mean, S , is the sample logarithmic SD and, k , is the station skew coefficient (Flynn et al., 2006). The average percent difference between Weibull and PeakFQ results were 33% for the 2-year return period and 41% for the 10-year return period. The two methods were averaged to form a statistical representation of the observed peak streamflow for each watershed for the 2- and 10-year return periods.

3.3.2 | Rowe, Countryman, and Storey

Rowe et al. (1949) undertook extensive observations across southern California watersheds (Mexican border to San Luis Obispo) and developed relations for size of peak streamflow events and erosion rates associated with normal (unburned) conditions for 256 watersheds within five climatic zones. Relations were established between storm precipitation and post-fire peak discharge for watersheds from the years 1869 to 1949 in each specific storm zone. It should be noted that several large storm events occurred after 1950 that were not recorded during the RCS study, which would have likely influenced the model significantly. The changes in these flows for subsequent post-fire years were determined and are the basis for the 256 LUTs. Since discharge measurements were not available for all watersheds, rating curves were established for each storm zone considering size, shape, steepness, stream channel characteristics, infiltration and water storage capacities of various soil-geologic formations, precipitation, and vegetation characteristics (Rowe et al., 1949). Each of the 256 tables were adjusted according to percent burnable area and vegetation density, and includes post-fire streamflow predictions for 1, 2, 3, 7, 15, 30 and 70 years (normal) after burning. The San Bernardino storm zone is the only region where RCS includes the influence of snowpack in streamflow estimates.

The RCS normal and burned peak streamflow estimates for the 33 watersheds were compared to the logarithmic means of the basic frequency classes (tables A and B of Rowe et al., 1949). A Savitzky-Golay function (Orfanidis, 1996) was used to remove noise from the data and to create a smooth curve for the storm frequency relationship. Data were plotted for 1, 2, 3, 7, 15, 30 and 70 years after the fire. Power functions were fitted to these relationships, where R^2 values were greater than 0.95, with the form:

$$Q = a \times p^b, \quad (6)$$

where Q is the predicted peak streamflow from RCS, a and b are coefficients, and p is the exceedance probability. Also, the RCS 1949 linear function was used to calculate the effect of partial burn on peak streamflow by proportioning with the percent of burnable area.

The 2- and 10-year recurrence interval predictions to assess watersheds are typically used by WERT and BAER teams because there is more confidence in flood flow prediction methods at smaller recurrence intervals

compared to larger intervals such as 25-, 50- 100-year (Kinoshita et al., 2014). Additionally, the recovery period for local vegetation in southern California is typically 2–7 years, which influences the hydrologic response (Bell et al., 2009; Keeley & Keeley, 1981; Kinoshita & Hogue, 2011). Thus, our post-fire predictions were derived from available streamflow observations collected within the first 7 years after fire for all of the watersheds.

3.3.3 | Random forest post-fire model

Random forests (RF) are an effective machine learning (ML) tool for prediction, both in classification problems and regression (Breiman, 2001). We developed two random forest models to predict post-fire peak streamflow. The MATLAB R2019a RF TreeBagger function combines the results of many decision trees (without replacement) and was used to build a regression based on the 45 watershed parameters, RF-45. The sample size was increased from 33 to 74 by selecting one to three post-fire storm events for each watershed. In general, tree-structured classifiers are independently distributed and explore different class conditions at each input. One of the main advantages of random forest is reproducibility and high transparency of feature importance. Random forests' feature importance is easy to interpret directly from the model, allowing conclusions to be drawn for the impact of different watershed parameters on the accuracy of predictions. TreeBagger also requires a low amount of hyperparameter tuning and the features do not need to fit a normal distribution, which is present in post-fire peak flow data. However, a common issue when building an RF model is the tendency for models to over-fit to the data, translating to a smaller variance in the predictions. This can occur if there are too many features in the regression, which falsely implies that the model is predicting perfectly. TreeBagger helped to reduce overfitting of data by using Bootstrap-aggregated (bagged) decision trees, which combined the results of many decision trees, where the Strong Law of Large Numbers applied (Feller, 1968; Pal, 2005). We also filtered out redundant or unimportant parameters, resulting in a multi-variable model with only five important parameters to predict post-fire peak streamflow (RF-5). RF-5 was validated using a k-fold cross validation with $k = 5$. The accuracy of both random forest models were assessed for each region and each watershed by using root mean squared error and coefficient of determination [Equations (2) and (3)] to evaluate model performance in comparison to observed streamflow data. The most important parameters identified by ML were also used to create a regression model using a three-dimensional polynomial function.

4 | RESULTS

4.1 | Rowe Countryman and Storey

4.1.1 | RCS performance before fire

Only 24 of the 33 watersheds had observed pre-fire streamflow, which are shown as streamflow per unit area for the 2- and 10-year recurrence interval events (Figure 2). Pre-fire, RCS over-predicted the

2-year return period for 17 of the watersheds and under-predicted the 10-year return period for 18 of the watersheds. In total, the 2-year return period had a positive bias of 0.162 cms/km^2 and the 10-year return period had a negative bias of -0.791 cms/km^2 (Table 2). There was substantial variation between watersheds that the RCS method did not represent. For example, the SD for the RCS 10-year return period was 0.31 cms/km^2 , while the SD of the observed 10-year return period was 1.28 cms/km^2 (Figure 2). The Santa Ynez region had the lowest accuracy by region for the 10-year return period, bias = -2.362 cms/km^2 , and Franklin Canyon, within the Santa Ynez region, had the lowest accuracy for all watersheds, where 10-year return period peak flow was under-predicted by a factor of 4.75. Overall, pre-fire peak streamflow prediction performance was low for the 2- and 10-year recurrence interval events ($R^2 = 0.24$ and $\text{RMSE} = 0.38 \text{ cms/km}^2$; $R^2 = 0.34$ and $\text{RMSE} = 1.43 \text{ cms/km}^2$, respectively).

4.1.2 | RCS performance after fire

For 10-year return period post-fire predictions, 22 watersheds experienced flooding during the first 5 years after fire and were under-predicted by RCS. When comparing observed post-fire flow directly to the probabilistic predictions, we found R^2 and RMSE for RCS 2-year return periods yielded 0.26 and 16.01 cms/km^2 , and R^2 and RMSE for RCS 10-year return periods yielded 0.25 and 15.52 cms/km^2 , respectively. Predictions generally had largely negative bias with 2-year return periods yielding bias of -8.68 cms/km^2 and 10-year return periods yielding bias of -7.78 cms/km^2 . Regionally, it was noted that 13 watersheds observed post-fire peak streamflow larger than the RCS 100-year prediction. Watersheds in the San Diego and San Jacinto regions on average had 149% lower post-fire peak streamflow compared to the other regions. Predictions for watersheds in the Santa Ynez, San Gabriel, San Bernardino, and Santa Ana mountains were inaccurate, with errors ranging up to 1720% during the floods at Dickey Canyon that followed the 2018 Holy Fire (Figure 3). These flows were rapid, where field observed velocity was measured to be approximately 12 m/s.

4.2 | Random forest post-fire model performance

The RF-45 TreeBagger function identified the following parameters as the most important for predicting post-fire peak streamflow for the study area (in order of importance): days elapsed from end of fire (containment date) to storm, total area of watershed burned, watershed drainage area, watershed perimeter, and peak 1-hour rainfall intensity (Figure S1). A second RF model was developed using only the five most important parameters. This resulted in a model that could be adequately represented with five parameters, therefore eliminating the issue of model overfitting (Figure 4). The RF-45 ($R^2 = 0.79$ and $\text{RMSE} = 7.34 \text{ cms/km}^2$) and RF-5 models ($R^2 = 0.46$ and $\text{RMSE} = 7.89 \text{ cms/km}^2$) performed better than the RCS method.

Accuracy decreased substantially when peak streamflows were above 10 cms/km^2 , most likely due to uncertainty caused by debris

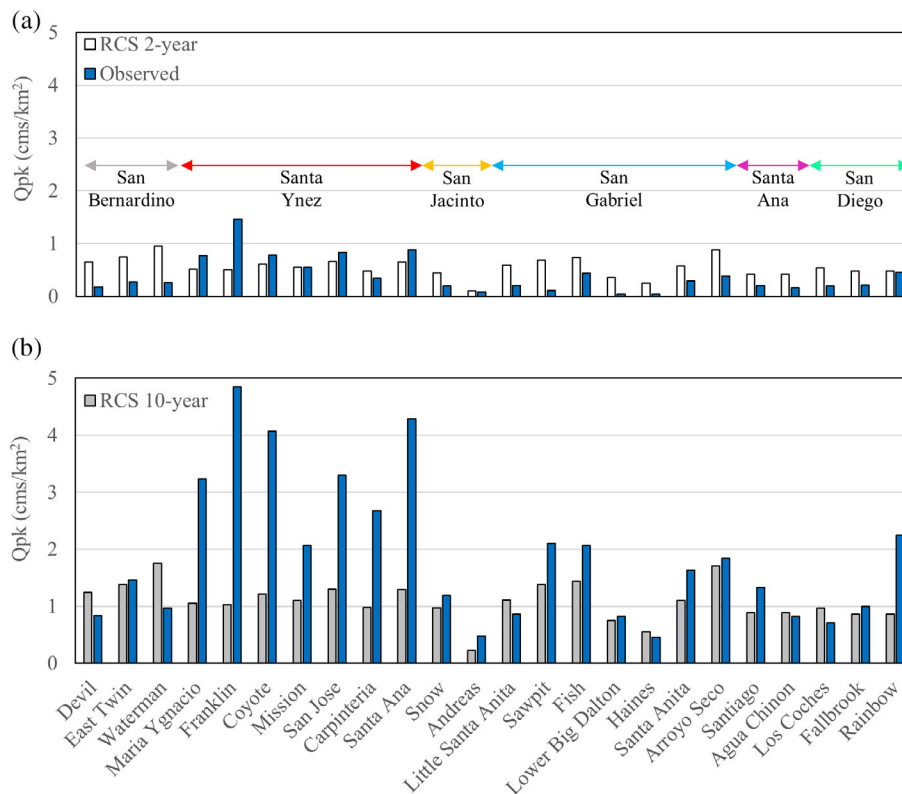


FIGURE 2 Rowe, Countryman, and Storey (RCS) unburned peak streamflow predictions compared to observed peak streamflow for 2-year (a) and 10-year (b) return periods

TABLE 2 Rowe, Countryman, and Storey (RCS) bias for peak streamflow predictions by region for the 2- and 10-year events

Region	RCS Bias (cms/km ²)	
	Q2	Q10
San Bernardino (n = 3)	0.551	0.371
Santa Ynez (n = 7)	−0.238	−2.362
San Jacinto (n = 2)	0.134	−0.237
San Gabriel (n = 6)	0.346	0.230
Santa Ana (n = 2)	0.237	−0.188
San Diego (n = 4)	0.272	−0.276
Southern California (n = 24)	0.162	−0.791

Note: Return periods were calculated from at least 21 years of peak flow data and n represents the number of watersheds.

flows and hyperconcentrated flows. The Santa Ynez region had the highest R^2 compared to the other regions (Bias = -1.77 cms/km²; $R^2 = 0.93$; RMSE = 7.99 cms/km²). This region also had the largest sample size in our study ($n = 27$) and the largest amount of available precipitation data to train the RF model.

Additionally, we compared the performance of RCS and RF-5 for the largest post-fire floods for each of the 33 watersheds between 1920–2018 (Figure 5). The RCS 2-year and RCS 10-year RMSE values were 16.01 cms/km² and 15.52 cms/km², respectively, while the RF RMSE was found to be lower at 10.41 cms/km².

4.3 | Towards an analytical solution for assessing post-fire peak flows

In June 2020, 65 out of 116 researchers and professionals in fire science prioritized “assessing and mitigating flash flood and debris flows hazards” over “burn area recovery” ($n = 31$), “water quality impacts” ($n = 17$), and “invasive species and/or changes in fire regime” ($n = 3$) (Coalitions, & Collaboratives, Inc., 2020). This motivated the development of a simple analytical solution for assessing immediate responses for post-fire peak flows in small watersheds. The most important parameters identified by RF-45 were time after fire (used to distinguish events within the first year), rainfall intensity, and burned area; they were used to create a simple regression (Figure 6). Thirty-one rainfall-runoff events during the first year after fire from the study area were fitted to a three-dimensional polynomial function ($R^2 = 0.82$) with the equation:

$$Qpk = -8.316 + 0.4033(A) + 0.9041(i60) - 0.04079(A)(i60) + 0.0127(i60)^2, \quad (7)$$

where Qpk is peak streamflow (cms/km²), A is burned area (km²), and i60 is peak hourly rainfall intensity (mm/h). Watershed area and watershed perimeter were not used for the regression. On average, burn proportions consisted of 56% moderate to high soil burn severity and 44% unburned to low soil burn severity.



FIGURE 3 Sediment-laden flows and high water mark observations in a concrete lined channel at Toft Dr. near the outlet of Dickey Canyon during 29 November (a and b) and 6 December 2018 storms (c). The December 6 peak flow filled the channel (c) and resulted in damage at outlet, where flow exceeded the culvert capacity (d). Photos a and c were extracted from videos provided by Riverside County Flood Control and Water Conservation District personnel and by resident S. Engelhardt, respectively

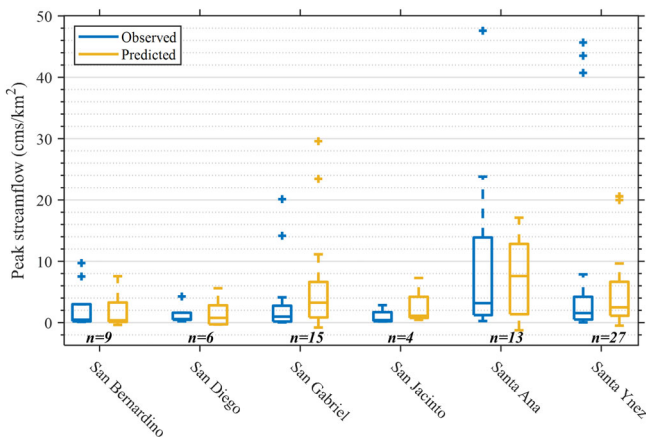


FIGURE 4 Predictions for the RF-5 random forest model by region. The sample size (n) is noted for each region

5 | DISCUSSION

5.1 | The future role of Rowe, Countryman, and Storey

RCS is commonly used in southern California after wildfire to model flood risk for affected watersheds. In this study, RCS had large inaccuracy for small to medium-sized watersheds (1 to 42 km²). This could be due to a multitude of factors including watershed morphology, exclusion of soil burn severity, greater development in the wildland-

urban interface, and increasing frequency in extreme weather events due to climate change. RCS had the largest inaccuracies for watersheds in the Santa Ynez Mountains, which is of concern due to the tendency for hazardous (Sections 2.1–2.3) events in this region, such as the 9 January 2018 Montecito debris flows (Kean et al., 2019). RCS regressions were developed for flows with low sediment concentrations (non-bulked flows), therefore, RCS predictions are expected to be limited and unable to predict peak flows associated with debris flows. In comparison to clear water flows, which generally have suspended-sediment concentrations less than 5% to 10% sediment by volume, hyperconcentrated flows can have suspended-sediment concentrations from 5% to 60% sediment by volume, and debris flows can have suspended-sediment concentrations greater than 60% sediment by volume (Pierson, 2005). Accurate predictions of post-fire streamflow along the continuum from flooding to debris flows are needed due to their frequent occurrence following wildfire in southern California (Cannon & DeGraff, 2009).

Significant advances in post-fire hydrology since the development of Rowe et al. (1949) should be incorporated to improve the accuracy of predictions (Kinoshita et al., 2014). For example, sediment bulking is implicit in RCS, yet independent variables that are strongly linked to sediment production or sediment yield are not used. Additionally, this observation-based method predates development of the soil burn severity metric. Soil burn severity characterizes the fire-induced changes in soil and ground cover properties that can affect infiltration, runoff, and erosion potential (Parsons et al., 2010) and is incorporated

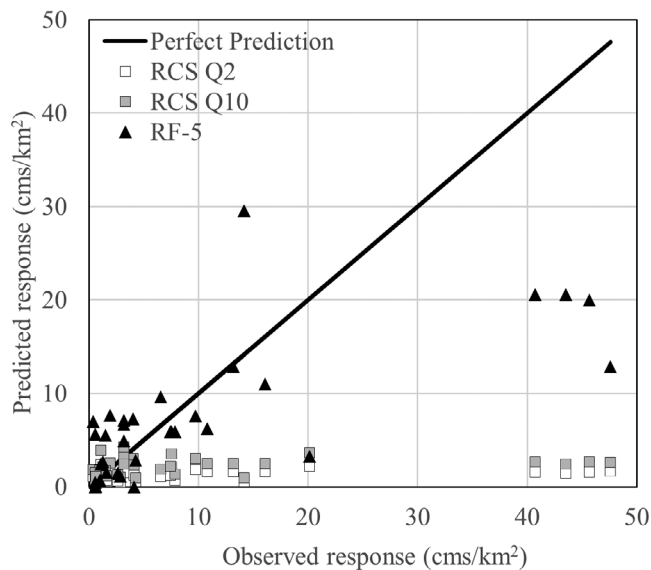


FIGURE 5 Observed peak streamflow versus predicted streamflow response. The black line represents a perfect prediction. Squares represent RCS (2- and 10-year events) and triangles represent random forest with the five most important parameters (RF-5). RF-5 is based on the entire training dataset and has no affiliated event magnitude. The extreme conditions or the highest floods for each watershed are shown ($n = 33$)

in post-fire hydrogeomorphic modelling as an independent variable to predict debris flows and debris yield (Gartner et al., 2014; Staley et al., 2017).

Pre-fire RCS SDs between watersheds (0.17–0.31 cms/km²) were smaller than the observed estimates (0.35–1.28 cms/km²), indicating that RCS predicted less variation than was actually present. This disparity between the SDs highlights the insensitivity of RCS predictions to different conditions between watersheds, and ultimately, contributes to additional error in post-fire predictions. The post-fire RCS method utilizes “fire factors” that modify pre-fire flow. This discrepancy is illustrated in our post-fire predictions of the Santa Ynez region.

Many of the spatially and temporally sensitive parameters such as rainfall intensity and soil burn severity are not adequately represented

in the RCS 1949 method. The limitations of RCS are attributed to its conceptualization prior to the development of the Geographic Information System (GIS). While, RCS rating curves were developed using basin size, shape, steepness, stream channel characteristics, infiltration and water storage capacities of various soil-geologic formations, precipitation, and vegetation characteristics (Rowe et al., 1949), these datasets were based on hand-drawn maps, field observations, and other historical records with lower spatial and temporal resolution. Further, RCS used a flood frequency technique that assumes a static landscape and climate; however, these assumptions are not valid under dynamic climate (Milly et al., 2008). For example, studies such as Musselman et al. (2017) and Prein et al. (2017) note that climate is not stationary, where earlier onset of snowmelt, increased air and water temperature, and increased frequency of extreme weather events can directly impact surface runoff. Therefore, a statistical, flood frequency approach to post-fire modelling, or a model that uses return periods and probabilities of occurrence such as RCS, will decrease in reliability over time, eventually rendering it irrelevant for future post-fire risk assessment in southern California.

5.2 | Role of machine learning as a tool for post-fire risk assessment

The parameters presented in this study (see Data Availability Statement) are essential in characterizing post-fire response in small southern California watersheds, however, this list is not exhaustive and potentially misses other important parameters. For example, 15-minute and 30-minute peak rainfall intensities, vegetation density, vegetation type, soil moisture, fault boundaries, sediment availability in the channels, relative humidity, and drought and climate variations, were not investigated (DiBiase & Lamb, 2020). Also, RF-45 did not determine soil burn severity to be an important parameter, which is contrary to several studies that note the importance of soil burn severity in triggering large post-fire peak flows (Gartner et al., 2014; Huffman et al., 2001; Lewis et al., 2006; Moody, 2012; Shakesby et al., 2016; Staley et al., 2017). This discrepancy is likely due to the lack of soil burn severity data for our modelling exercise. Soil burn severity was not available for 35 of the 74 rainfall-runoff events,

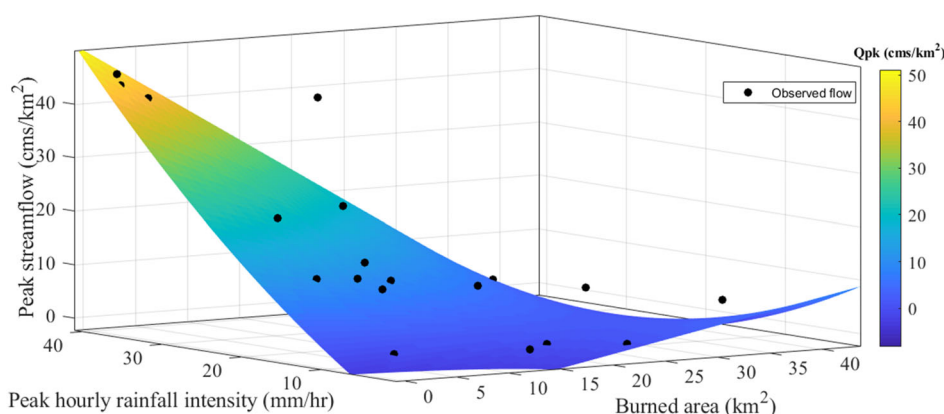


FIGURE 6 Modelled regression for small, steep catchments during the first year after fire in southern California, fitted to historic high flows within the first year after wildfire collected from 1920–2019. This model is limited to watersheds ranging between 1 to 20 km² where more than half of the watershed has been burned at moderate to high soil burn severity

limiting the model's ability to identify the importance of severity. This reinforces the need and importance for consistent collection of field data, particularly high temporal resolution rainfall intensity, soil burn severity mapping, and streamflow data (Staley et al., 2013) to improve the contributions of ML in post-fire hydrologic predictions.

There is significant research that demonstrates the importance of high temporal resolution rainfall data (e.g., 5-, 15-, and 30-minute rainfall intensities) initiating debris flows and associated high peak flows (Staley et al., 2013). This study focused on data that were open access (60-minute rainfall intensity). Further, only one rain gauge was used as a representative rainfall measurement for each watershed, which may contribute to uncertainty in the RF-5, RF-45, and polynomial regression predictions. There are also inherent errors in the measured post-fire peak streamflow, which may have been heavily laden with soil, ash, burned vegetation, large boulders, and other debris (i.e., significantly bulked flow).

This study suggests that with sufficient high-quality data, machine learning can be a valuable procedure for developing predictive tools for post-fire risk assessment. For example, the Santa Ynez region had the largest sample size and the most available rainfall data, resulting in the highest R^2 by region for RF-5 ($n = 27$; Bias = -1.77 cms/km²; $R^2 = 0.93$; RMSE = 7.99 cms/km²). Further, machine learning requires data collection, calibration, and parameterization that should be carried out cautiously. Excluding or missing parameters that have significant importance to model accuracy can lead to highly inaccurate predictions due to insufficient processes being defined by the data.

5.3 | Factors influencing post-fire peak streamflow

Based upon our ML approach, peak rainfall intensity, watershed size, and time after fire containment have a significant role in determining flow rate per unit area after wildfire (Figure 7). We observed that peak hourly rainfall intensities over 10 mm/h led to larger magnitude floods (Figure 7(a)). These findings may be due to physical watershed processes, whereby larger peak rainfall intensities increase rill erosion and channel incision (Cannon & DeGraff, 2009). Watersheds with smaller areas (1–10 km²) are more likely to have larger magnitude runoff per unit area ($p < 0.05$) (Figure 7(b)), which is similar to Neary et al. (2005). In smaller watersheds with predominantly chaparral vegetation type, runoff responses are erratic and have potential to transport large amounts of sediment per unit area after fire (Keller et al., 1997). Neary et al. (2005) also reported much larger magnitudes for small watersheds in Western United States (<1 km²), where post-fire peak flows averaged 193 cms/km², further highlighting the increased potential for higher magnitude peak flows. Finally, storms that occurred closer in time to the fire containment have a higher likelihood of larger magnitude events ($p < 0.05$) (Figure 7(c)). The passing of time allows hydrophobic soils to normalize and vegetation to recover, reducing rainfall impact on bare soil (Neary et al., 2005).

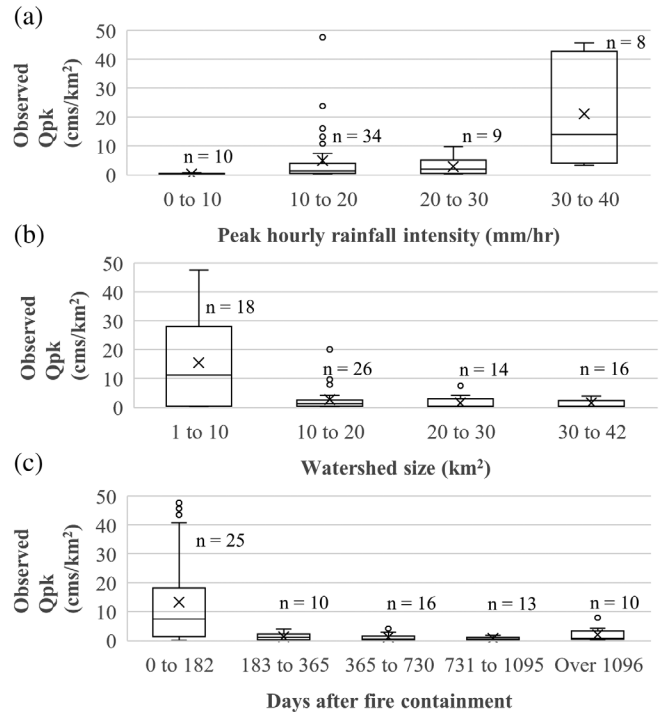


FIGURE 7 Observed peak streamflow per unit area with respect to peak hourly rainfall intensities (a), watershed size (b), and days after fire containment (c)

5.4 | Analytical solution

Rapid assessment and accurate modelling of post-fire peak streamflow are essential for effective risk management implementation. The use of RCS has persisted in emergency assessments despite its shortcomings due to general acceptance, ease of use, and lack of a better simplified model. Many current models require extensive data acquisition, model setup and testing, and field calibration; these models may generally work well but are not feasible under time constraints required by post-fire assessment teams and emergency management agencies to make rapid decisions for quantifying risk and developing response measures. Thus, we advocate that more work is needed to provide more data for validation and improve existing methods and tools that better fit the current needs of post-fire assessment teams and local agencies to quantify risk to downstream communities, infrastructure, and ecosystems. Based on our regional analysis using random forest (Figure 4; Figure S1), we propose a simple regression that can be used for peak streamflow estimates in post-fire risk assessment for the first year after fire for watersheds between 1 to 20 km² in southern California [Figure 6; Equation (7)].

6 | CONCLUSION

Following wildfires in southern California, the probability of flooding and debris flows increase, thus prompting the need for accurate

prediction to protect downstream communities, infrastructure, and ecosystems. Rowe et al. (1949) produced large inaccuracies for pre- and post-fire peak streamflow predictions in small to medium-sized watersheds (1 to 42 km²) in southern California. We suggest that RCS should be used with extreme caution. We demonstrate the development of two models using machine learning. We showed that RF-45 can identify relationships and characterize post-fire peak streamflow of small watersheds. Through RF-45, it was discovered that days elapsed from end of fire to storm, total area of watershed burned, watershed drainage area, watershed perimeter, and peak 1-hour rainfall intensity are important parameters that contribute to greater model accuracy. The RF-5 model built with these five parameters (Bias = -2.81 cms/km²; R² = 0.46; RMSE = 7.89 cms/km²) was more accurate than the RCS Q2 and Q10 regressions (Bias = -8.68 - -7.78 cms/km²; R² = 0.26-0.25; RMSE = 15.52-16.01 cms/km²). A simple analytical solution is introduced to provide post-fire assessment teams an interim tool to rapidly predict peak floods for small watersheds in southern California (Bias = -2.26 cms/km²; R² = 0.82; RMSE = 6.59 cms/km²). We conclude that a significant increase in data collection of high temporal and spatial resolution rainfall intensity, streamflow, and sediment loading in channels will help to guide future model development to quantify post-fire flood risk.

ACKNOWLEDGEMENTS

This work is partially supported by the Joint Fire Science Program Graduate Research Innovation Award (#19-1-01-55) and Department of Conservation - California Geological Survey. We thank Dr. Kinoshita's Disturbance Hydrology Lab for insightful discussions, and students, Harmit Chima, Ubaldo Gonzalez, and Sydney Johnson from the Mathematics, Engineering, Science Achievement (MESA) 2019 Research Academy at San Diego State University for their contributions. We also appreciate the United States Forest Service hydrologists, UC Riverside researchers, Jason Uhley and multiple support staff at the Riverside County Flood Control and Water Conservation District, and local residents including Dale Hook, Peter Rasinski, Shannon Akins, and Sue Engelhardt for sharing observations and findings following the 2018 Holy Fire. The authors of this work would also like to acknowledge that some of the data collected from this study came from lands belonging to the Pechanga Band of Luiseño Indians and the Agua Caliente Band of Cahuilla Indians. In particular, data were collected for areas affected by the 1980 Dry Falls Fire, the 2000 Pechanga Fire, and the 2013 Mountain Fire. We recognize the continuing and long-lasting presence of all indigenous groups of this land.

DATA AVAILABILITY STATEMENT

The data that support the findings of this study are openly available at HydroShare (<https://www.hydroshare.org/resource/9e38375a19cf4355aac466ccd78e8282/>).

ORCID

Brenton A. Wilder  <https://orcid.org/0000-0003-3340-7862>
 Alicia M. Kinoshita  <https://orcid.org/0000-0002-2283-4490>

REFERENCES

- Bell, C. E., Ditomaso, J. M., & Brooks, M. L. (2009). *Invasive plants and wild-fires in Southern California*, Publication 8397, Davis, CA: UCANR.
- Biddinger, T., Gallegos, A., Janeki, A., TenPas, J., & Weaver, R. (2003). *BAER watershed assessment report, 2003 Grand Prix and Old Fire*. San Bernardino National Forest, unpublished report.
- Breiman, L. (2001). Random forests. *Machine Learning*, 45(1), 5-32.
- Cannon, S. H., & DeGraff, J. (2009). The increasing wildfire and post-fire debris-flow threat in western USA, and implications for consequences of climate change. In K. Sassa & P. Canuti (Eds.), *Landslides-disaster risk reduction* (pp. 177-190). Springer.
- Cannon, S. H., Gartner, J. E., Rupert, M. G., & Michael, J. A. (2004). *Emergency assessment of debris-flow hazards from basins burned by the Padua fire of 2003, Southern California*. US Geological Survey Open-File Report, 1072, 14.
- Cannon, S. H., Gartner, J. E., Wilson, R. C., Bowers, J. C., & Laber, J. L. (2008). Storm rainfall conditions for floods and debris flows from recently burned areas in southwestern Colorado and southern California. *Geomorphology*, 96(3-4), 250-269.
- CGS (California Geological Survey). (2002). California geomorphic provinces, Note 36. Sacramento, CA. p. 4.
- CGS (California Geological Survey). (2018). *Geology of California*. Sacramento, CA.
- Chawner, W. D. (1935). Alluvial fan flooding: The Montrose, California, flood of 1934. *Geographical Review*, 25(2), 255-263.
- Clarke, R. T. (2002). Estimating trends in data from the Weibull and a generalized extreme value distribution. *Water Resources Research*, 38(6), 25-1-25-10.
- Cleland, D., Freeouf, J., Keys, J., Nowacki, G., Carpenter, C., & McNab, W. (2007). *Ecological subregions: Sections and subsections for the conterminous United States*. General Technical Report WO-76D, 76.
- Coalitions & Collaboratives, Inc. (Producer). (2020). *After the Flames* [Video]. Retrieved from <https://aftertheflames.com/science-session-resources/>
- DeBano, L. F. (2000). The role of fire and soil heating on water repellency in wildland environments: A review. *Journal of Hydrology*, 231, 195-206.
- Dettinger, M. (2011). Climate change, atmospheric rivers, and floods in California-A multimodel analysis of storm frequency and magnitude changes 1. *JAWRA Journal of the American Water Resources Association*, 47(3), 514-523.
- DiBiase, R. A., & Lamb, M. P. (2020). Dry sediment loading of headwater channels fuels post-wildfire debris flows in bedrock landscapes. *Geology*, 48(2), 189-193.
- Doerr, S., Shakesby, R., & Walsh, R. (2000). Soil water repellency: Its causes, characteristics and hydro-geomorphological significance. *Earth-Science Reviews*, 51(1-4), 33-65.
- Doerr, S. H., Shakesby, R. A., & MacDonald, L. H. (2009). Soil water repellency: A key factor in post-fire erosion. C. Artemi & P.R. Robichaud In *Fire effects on soils and restoration strategies* (pp. 213-240). CRC Press.
- Feller, W. (1968). *An introduction to probability theory and its applications* (Vol. 1). John Wiley & Sons.
- Flynn, K. M., Kirby, W. H., & Hummel, P. R. (2006). *User's manual for program PeakFQ, annual flood-frequency analysis using Bulletin 17B guidelines* (No. 4-B4).
- Foltz, R. B., Robiochaud, P. R., & Rhee, H. (2009). *A synthesis of post-fire road treatments for BAER teams: Methods, treatment effectiveness, and decisionmaking tools for rehabilitation*. Gen. Technical Report RMRS-GTR-228. Fort Collins, CO: U.S. Department of Agriculture, Forest Service, Rocky Mountain Research Station, p. 152.
- FRAP (Fire and Resource Assessment Program). (2015). State fire perimeter database. California Department of Forestry and Fire Protection. Sacramento, CA.
- FRAP (Fire and Resource Assessment Program). (2018). California's forests and rangelands: 2017 assessment. California Department of Forestry and Fire Protection. Sacramento, CA, p. 304.

- Gartner, J. E., Cannon, S. H., & Santi, P. M. (2014). Empirical models for predicting volumes of sediment deposited by debris flows and sediment-laden floods in the transverse ranges of southern California. *Engineering Geology*, 176, 45–56.
- Harden, J. W., & Matti, J. C. (1989). Holocene and late Pleistocene slip rates on the San Andreas fault in Yucaipa, California, using displaced alluvial-fan deposits and soil chronology. *Geological Society of America Bulletin*, 101(9), 1107–1117.
- Huffman, E. L., MacDonald, L. H., & Stednick, J. D. (2001). Strength and persistence of fire-induced soil hydrophobicity under ponderosa and lodgepole pine, Colorado Front Range. *Hydrological Processes*, 15(15), 2877–2892.
- Kean, J. W., Staley, D. M., Lancaster, J. T., Rengers, F. K., Swanson, B. J., Coe, J. A., Hernandez, J. L., Sigman, A. J., Allstadt, K. E., & Lindsay, D. N. (2019). Inundation, flow dynamics, and damage in the 9 January 2018 Montecito debris-flow event, California, USA: Opportunities and challenges for post-wildfire risk assessment. *Geosphere*, 15(4), 1140–1163.
- Keeley, J. E. (2009). Fire intensity, fire severity and burn severity: A brief review and suggested usage. *International Journal of Wildland Fire*, 18(1), 116–126.
- Keeley, J. E., Fotheringham, C., & Moritz, M. A. (2004). Lessons from the October 2003. Wildfires in Southern California. *Journal of Forestry*, 102(7), 26–31.
- Keeley, J. E., & Keeley, S. C. (1981). Post-fire regeneration of southern California chaparral. *American Journal of Botany*, 68(4), 524–530.
- Keller, E. A., Valentine, D. W., & Gibbs, D. R. (1997). Hydrological response of small watersheds following the Southern California Painted Cave Fire of June 1990. *Hydrological Processes*, 11(4), 401–414.
- Kinoshita, A. M., Chin, A., Simon, G. L., Briles, C., Hogue, T. S., O'Dowd, A. P., Gerlak, A.K., & Albornoz, A.U. (2016). Wildfire, water, and society: Toward integrative research in the “Anthropocene”. *Anthropocene*, 16, 16–27.
- Kinoshita, A. M., & Hogue, T. S. (2011). Spatial and temporal controls on post-fire hydrologic recovery in Southern California watersheds. *CATENA*, 87(2), 240–252.
- Kinoshita, A. M., Hogue, T. S., & Napper, C. (2014). Evaluating pre-and post-fire peak discharge predictions across western US watersheds. *JAWRA Journal of the American Water Resources Association*, 50(6), 1540–1557.
- Lamjiri, M. A., Dettinger, M. D., Ralph, F. M., Oakley, N. S., & Rutz, J. J. (2018). Hourly analyses of the large storms and atmospheric rivers that provide most of California's precipitation in only 10 to 100 hours per year. *San Francisco Estuary and Watershed Science*, 16(4), 1–17.
- Lancaster, J. T., Swanson, B. J., Lukashova, S., Oakley, N., Lee, J. B., Spangler, E., Hernandez, J. L., Olson, B. P. E., DeFrisco, M. J., Lindsay, D. J., Schwartz, Y. J., McCrea, S. E., Roffers, P. D., & C.M. Tran. (in press). Observations and analyses of the 9 January 2018 debris flow disaster, Santa Barbara County. Environmental and Engineering Geoscience.
- Lavé, J., & Burbank, D. (2004). Denudation processes and rates in the Transverse Ranges, southern California: Erosional response of a transitional landscape to external and anthropogenic forcing. *Journal of Geophysical Research: Earth Surface*, 109, F01006.
- Lewis, S. A., Wu, J. Q., & Robichaud, P. R. (2006). Assessing burn severity and comparing soil water repellency, Hayman Fire, Colorado. *Hydrological Processes: An International Journal*, 20(1), 1–16.
- Miller, N. L., & Schlegel, N. J. (2006). Climate change projected fire weather sensitivity: California Santa Ana wind occurrence. *Geophysical Research Letters*, 33(L15711), 1–5.
- Milly, P. C., Betancourt, J., Falkenmark, M., Hirsch, R. M., Kundzewicz, Z. W., Lettenmaier, D. P., & Stouffer, R. J. (2008). Stationarity is dead: Whither water management? *Science*, 319(5863), 573–574.
- Moody, J. A. (2012). *An analytical method for predicting postwildfire peak discharges*. DOI USGS Investigations Report, 5236.
- Moody, J. A., & Martin, D. A. (2001). Initial hydrologic and geomorphic response following a wildfire in the Colorado Front Range. *Earth Surface Processes and Landforms: The Journal of the British Geomorphological Research Group*, 26(10), 1049–1070.
- Moody, J. A., Shakesby, R. A., Robichaud, P. R., Cannon, S. H., & Martin, D. A. (2013). Current research issues related to post-wildfire runoff and erosion processes. *Earth-Science Reviews*, 122, 10–37.
- Moore, M., Bigginger, T., Thornton, J., Wright, K., & Stewart, C. (2009). *BAER watershed assessment report, Station Fire*. Angeles National Forest, unpublished report.
- Musselman, K. N., Molotch, N. P., & Margulis, S. A. (2017). Snowmelt response to simulated warming across a large elevation gradient, southern Sierra Nevada, California. *The Cryosphere*, 11(6), 2847–2866.
- Neary, D. G., Ryan, K. C., & DeBano, L. F. (2005). *Wildland fire in ecosystems: Effects of fire on soils and water*. Gen. Tech. Rep. RMRS-GTR-42-vol. 4. Ogden, UT: US Department of Agriculture, Forest Service, Rocky Mountain Research Station. p. 250, 42.
- Neiman, P. J., Ralph, F. M., Wick, G. A., Kuo, Y. H., Wee, T. K., Ma, Z., Taylor, G. H., & Dettinger, M. D. (2008). Diagnosis of an intense atmospheric river impacting the Pacific Northwest: Storm summary and off-shore vertical structure observed with COSMIC satellite retrievals. *Monthly Weather Review*, 136(11), 4398–4420.
- Oakley, N. S., Lancaster, J. T., Kaplan, M. L., & Ralph, F. M. (2017). Synoptic conditions associated with cool season post-fire debris flows in the Transverse Ranges of southern California. *Natural Hazards*, 88(1), 327–354.
- O'Connor, J. E., & Costa, J. E. (2004). *The world's largest floods, past and present: Their causes and magnitudes* (No. 1254). Geological Survey (USGS).
- Orfanidis, S. J. (1996). *Introduction to signal processing*. Prentice Hall.
- Pal, M. (2005). Random forest classifier for remote sensing classification. *International Journal of Remote Sensing*, 26(1), 217–222.
- Parrett, C., Veilleux, A., Stedinger, J. R., Barth, N. A., Knifong, D. L., & Ferris, J. C. (2011). *Regional skew for California, and flood frequency for selected sites in the Sacramento-San Joaquin River Basin, based on data through water year 2006*. U. S. Geological Survey.
- Parsons, A., Robichaud, P. R., Lewis, S. A., Napper, C., & Clark, J. T. (2010). *Field guide for mapping post-fire soil burn severity*. Gen. Tech. Rep. RMRS-GTR-243. Fort Collins, CO: US Department of Agriculture, Forest Service, Rocky Mountain Research Station. p. 49, 243.
- Pierson, T. C. (2005). *Distinguishing between debris flows and floods from field evidence in small watersheds* (No. 2004-3142). U.S. Geological Survey Fact Sheet 2004-3142, p. 4.
- Prein, A. F., Rasmussen, R. M., Ikeda, K., Liu, C., Clark, M. P., & Holland, G. J. (2017). The future intensification of hourly precipitation extremes. *Nature Climate Change*, 7(1), 48–52.
- Radeloff, V. C., Hammer, R. B., Stewart, S. I., Fried, J. S., Holcomb, S. S., & McKeefry, J. F. (2005). The wildland-urban interface in the United States. *Ecological Applications*, 15(3), 799–805.
- Ralph, F. M., & Dettinger, M. D. (2012). Historical and national perspectives on extreme West Coast precipitation associated with atmospheric rivers during December 2010. *Bulletin of the American Meteorological Society*, 93(6), 783–790.
- Raphael, M. N. (2003). The Santa Ana winds of California. *Earth Interactions*, 7(8), 1–13.
- Robichaud, P. R., Elliot, W. J., Pierson, F. B., Hall, D. E., & Moffet, C. A. (2007). Predicting postfire erosion and mitigation effectiveness with a web-based probabilistic erosion model. *Catena*, 71(2), 229–241.
- Robichaud, P. R., Elliot, W. J., & Wagenbrenner, J. W. (2011, September). Probabilistic soil erosion modeling using the erosion risk management tool (ERMIT) after wildfires. In *International Symposium on Erosion and Landscape Evolution (ISELE)*, American Society of Agricultural and Biological Engineers, Anchorage, Alaska (p. 39).
- Rowe, P. B., Countryman, O. M., & Storey, H. C. (1949). *Probable peak discharges and erosion rates from southern California watersheds as influenced by fire*. US Department of Agriculture, Forest Service.

- Safford, H. D., & Van de Water, K. M. (2014). *Using fire return interval departure (FRID) analysis to map spatial and temporal changes in fire frequency on national forest lands in California*. Res. Pap. PSW-RP-266. Albany, CA: US Department of Agriculture, Forest Service, Pacific Southwest Research Station. p. 59, 266.
- Saxe, S., Hogue, T. S., & Hay, L. (2018). Characterization and evaluation of controls on post-fire streamflow response across western US watersheds. *Hydrology and Earth System Sciences*, 22(2), 1221–1237.
- Schmidt, L., Heße, F., Attinger, S., & Kumar, R. (2020). Challenges in applying machine learning models for hydrological inference: A case study for flooding events across Germany. *Water Resources Research*, 56.
- Scott, K. M., & Williams, R. P. (1978). *Erosion and sediment yields in the Transverse Ranges, southern California* (p. 38). US Government Printing Office.
- Shakesby, R. A., Moody, J. A., Martin, D. A., & Robichaud, P. R. (2016). Synthesising empirical results to improve predictions of post-wildfire runoff and erosion response. *International Journal of Wildland Fire*, 25(3), 257–261.
- Shurman, G., & Slosson, J. E. (1992). *Forensic engineering – Environmental case histories for engineers and geologists* (p. 296). Academic Press, Inc.
- Staley, D. M., Kean, J. W., Cannon, S. H., Schmidt, K. M., & Laber, J. L. (2013). Objective definition of rainfall intensity–duration thresholds for the initiation of post-fire debris flows in southern California. *Landslides*, 10(5), 547–562.
- Staley, D. M., Negri, J. A., Kean, J. W., Laber, J. L., Tillery, A. C., & Youberg, A. M. (2017). Prediction of spatially explicit rainfall intensity–duration thresholds for post-fire debris-flow generation in the western United States. *Geomorphology*, 278, 149–162.
- Syphard, A. D., Radeloff, V. C., Keeley, J. E., Hawbaker, T. J., Clayton, M. K., Stewart, S. I., & Hammer, R. B. (2007). Human influence on California fire regimes. *Ecological Applications*, 17(5), 1388–1402.
- Travis, B., Teal, M., & Gusman, J. (2012). Best methods and inherent limitations of bulked flow modeling with HEC-RAS. In *World Environmental and Water Resources Congress 2012: Crossing Boundaries* (pp. 1195–1202).
- Van de Water, K. M., & Safford, H. D. (2011). A summary of fire frequency estimates for California vegetation before Euro-American settlement. *Fire Ecology*, 7(3), 26–58.
- Wagenbrenner, J. W. (2013). *Post-fire stream channel processes: Changes in runoff rates, sediment delivery across spatial scales, and mitigation effectiveness*, PhD thesis, Pullman, WA: Washington State University.
- Wells, W. G., II. (1981). *Some effects of brushfires on erosion processes in coastal southern California*. In: Proceedings of a symposium on erosion and sediment transport in Pacific Rim steepplands. Publication No. 132. Christchurch, New Zealand: International Association of Hydrological Sciences, pp. 305–342.
- Wells, W. G. (1987). The effects of fire on the generation of debris flows in southern California. *Reviews in Engineering Geology*, 7, 105–114.
- WERT (Watershed Emergency Response Team). (2018a). Holy Fire—Watershed Emergency Response Team final report, CA-RRU-100160. Sacramento, CA, p. 83. plus appendices.
- WERT (Watershed Emergency Response Team). (2018b). Woolsey and Hill Fires—Watershed Emergency Response Team final report, CA-VNC-091023 and CA-VNC-090993. Sacramento, CA, p. 106. plus appendices.
- WERT (Watershed Emergency Response Team). (2019a). Saddle Ridge Fire—Watershed Emergency Response Team final report, CA-LFD-00001582. Sacramento, CA, p. 89. plus appendices.
- WERT (Watershed Emergency Response Team). (2019b). Cave Fire—Watershed Emergency Response Team final report, CA-LPF-002908. Sacramento, CA, p. 34. plus appendices.
- Westerling, A. L., Hidalgo, H. G., Cayan, D. R., & Swetnam, T. W. (2006). Warming and earlier spring increase western US forest wildfire activity. *Science*, 313(5789), 940–943.
- Williams, A. P., Abatzoglou, J. T., Gershunov, A., Guzman-Morales, J., Bishop, D. A., Balch, J. K., & Lettenmaier, D. P. (2019). Observed impacts of anthropogenic climate change on wildfire in California. *Earth's Future*, 7(8), 892–910.
- Wohlgemuth, P. (2016, March). Long-term hydrologic research on the San Dimas Experimental Forest, southern California: Lessons learned and future directions. In C. E. Stringer, K. W. Krauss, J. S. Latimer (Eds.), *Headwaters to estuaries: Advances in watershed science and management-Proceedings of the Fifth Interagency Conference on Research in the Watersheds*. North Charleston, SC. e-General Technical Report SRS-211. Asheville, NC: US Department of Agriculture Forest Service, Southern Research Station. 302 p. (Vol. 211, pp. 227–232).

SUPPORTING INFORMATION

Additional supporting information may be found online in the Supporting Information section at the end of this article.

How to cite this article: Wilder BA, Lancaster JT, Cafferata PH, et al. An analytical solution for rapidly predicting post-fire peak streamflow for small watersheds in southern California. *Hydrological Processes*. 2020;1–14. <https://doi.org/10.1002/hyp.13976>